energy&fuels

Article

Cite This: Energy Fuels 2019, 33, 4420−4431

pubs.acs.org/EF

Atmospheric Pressure Photoionization Fourier Transform Ion Cyclotron Resonance Mass Spectrometry Characterization of Oil Sand Process-Affected Water in Constructed Wetland Treatment

Chukwuemeka Ajaero,[†,‡] Kerry M. Peru,[‡] Sarah A. Hughes,[∥] Huan Chen,[⊥] Amy M. McKenna,[⊥] Yuri E. Corilo,[⊥] Dena W. McMartin,[*,†,#] and John V. Headley[‡]

[†]Environmental Systems Engineering, University of Regina, 3737 Wascana Parkway, Regina, Saskatchewan S4S 0A2, Canada

[‡]Watershed Hydrology and Ecology Research Division, Water Science and Technology Directorate, Environment and Climate Change Canada, 11 Innovation Boulevard, Saskatoon, Saskatchewan S7N 3H5, Canada

[∥]Shell Health—Americas, 150 N. Dairy Ashford Road, Houston, Texas 77079, United States

[⊥]National High Magnetic Field Laboratory, Florida State University, 1800 E. Paul Dirac Dr., Florida 32306, United States

[#]Department of Civil, Geological and Environmental Engineering, University of Saskatchewan, 57 Campus Drive, Saskatoon, Saskatchewan S7N 5A9, Canada

ABSTRACT: The remediation of oil sand process-affected water (OSPW) generated during the bitumen extraction in the oil sand region of Canada is an area of ongoing research interest. One of the primary remediation challenges is the removal of residual complex organic compounds present in the OSPW. In the present study, the molecular constitution of OSPW from aerated and nonaerated wetland treatments were characterized in constructed wetland treatment systems. Negative-ion and positive-ion atmospheric pressure photoionization (APPI) Fourier transform ion cyclotron resonance mass spectrometry (FT-ICR-MS) was used to provide extensive molecular-level analysis of the samples. Multiple aerated and nonaerated treatment wetland systems were characterized in terms of naphthenic acids (NAs), oxy-NAs, heteroatom NAs class, and double bond equivalent (DBE) versus carbon number to evaluate their molecular composition and variability. A broad range of heteroatom compound classes with variable relative abundances were identified. The DBE versus carbon number analysis revealed different levels of transformation of the compound classes, an indicator of NA fraction compound susceptibility to transformation. The selectivity and the extent of transformation of the compound classes were a function of the wetland design. The complementarity in the heteroatom classes detected in negative-ion and positive-ion APPI FT-ICR-MS highlight the need for multiple ionization methods for more complete coverage of the distribution of components in OSPW. The detailed molecular-level information can be useful for prediction of the fate and associated toxicity of the species and also treatment efficiencies of the wetland systems.

1. INTRODUCTION

Oil sands have attracted much attention because of the decline in conventional oil resources as much effort is focused toward the establishment of alternative sources of oil.[1] One of the largest deposits of oil sands in the world is found in Alberta, Canada.[2,3] The current method used to separate bitumen from oil sands by surface mining operations is based on the application of Clark alkali hot process, which generates large volumes of wastewater known as oil sand process-affected water (OSPW).[4−6] The OSPW is subsequently directed into large tailing ponds. Furthermore, OSPW in tailing ponds can mix with storm and surface water run-off, dyke drain water, groundwater, and connate water (water that is naturally part of the oil sands deposit), surface water, and shallow aquifer water removed during site construction prior to mining, consolidated tailings, fresh and aged OSPW, and water from wetland reclamation.[7−9] All these water that have made contact with oil sands are collectively considered as OSPW.[10] OSPW is a composition of a complex mixture of metals, semimetals, salts, and inorganic and organic compounds.[11−13] The organic constituents include classical naphthenic acids (NAs)/oxidized-NAs (oxy-NAs), aromatics, and heteroatom NAs such as nitrogen/sulfur/oxygen containing species.[14,15] Classical NAs, oxy-NAs, aromatics, and heteroatom NAs are generally described as NA fraction compounds (NAFCs).[16,17] The classical NA compounds are the primary toxic constituent found in OSPW.[8,18] The potential toxicity of other species in OSPW is not established, but some insights are emerging in the recent literature. For example, O_3S classes detected in negative electrospray ionization (ESI) were found to induce oxidative stress and damages on the cellular membranes of fission yeast (*Schizosaccharomyces pombe*) cells.[19] Other heteroatom NAFCs such as O_2S species detected by negative ionization mode were correlated to acute toxicity to fathead minnow (*Pimephales promelas*) embryos.[18,20] A recent study linked the obstruction of the conveyor proteins and the ATP-binding cassette (responsible for cleansing foreign substances in the body) primarily to sulfur and nitrogen-containing classes observed by the positive-ion ESI

Received: February 15, 2019
Revised: April 22, 2019
Published: April 23, 2019

DOI: 10.1021/acs.energyfuels.9b00469
Energy Fuels 2019, 33, 4420−4431

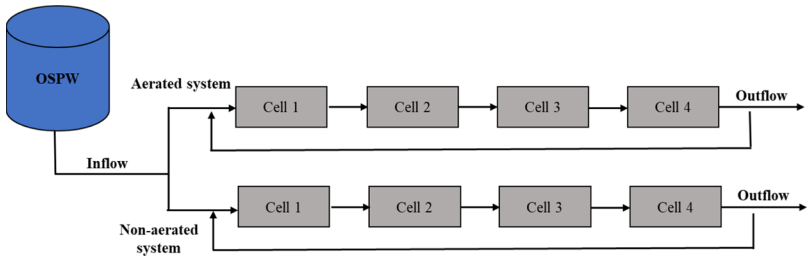

Figure 1. Modified schematic representation of the pilot CWT set up.

high-resolution Orbitrap mass spectrometry (MS).[21] Effect-directed analysis of OSPW found the nonacidic species of oxygen (O_2^+) observed using positive ionization mode to also cause acute toxicity.[18]

Remediation of OSPW has become an area of much interest[22−28] in which constructed wetland treatment (CWT) is an emerging and viable eco-technology.[29] The wetland designs are based primarily on the consortium of plants, soils, hydroperiods, and microbes for efficient remediation.[30,31] Developments in CWT technology are primarily focused on gaining knowledge of the fundamental processes in wetlands that can improve their performances.[32] Some studies demonstrated that specific transformation processes in treatment wetland such as oxidation could be promoted to improve the quality of wastewaters.[30,33] Constructed wetlands are characterized by specific conditions such as aerobic (aerated) and anaerobic (nonaerated) conditions that support different treatment processes for optimal removal of targeted compounds.[34] In aerated constructed wetlands, oxygen is increased to levels required for the degradation of contaminants.[35,36] The application of constructed wetlands has led to improved water quality. However, the analysis of NAFCs in such systems is prone to interferences from biological materials like fatty acids that can mask the characterization and quantification of NAFCs at the molecular level.

Studies on the characterization of NAs conducted with gas and liquid chromatography MS provide molecular-level information. However, their ability to address the fundamental problem of compositional coverage of OSPW is limited.[17] The complexity of the numerous chemical classes in OSPW presents a challenge concerning molecular-level characterization. Fourier transform ion cyclotron resonance (FT-ICR) MS is more appropriate for molecular-level characterization and extensive coverage of the compound classes in complex matrices than most other commonly used mass spectrometers based on the maximum mass resolution and accuracy that can be obtained for closely related ions.[37,38] Detailed composition of complex environmental matrices like OSPW using ultrahigh resolution MS has been successfully reported.[39,40] FT-ICR-MS offers ultrahigh resolution (about 500 000 resolution at 400 m/z) and accurate mass measurements (<1 ppm)[41,42] that facilitate unique compositional assignment of the many species found in OSPW samples.[39,40,43,44] Various ionization methods such as ESI and atmospheric pressure photoionization (APPI) coupled to FT-ICR-MS have been used to increase compositional coverage of OSPW.[14,40] On the other hand, some studies have highlighted the uniqueness of the APPI technique in the analysis of environmental samples[14,40,45,46] to provide additional knowledge on the specific degradation mechanism and transformation products in a complex heterogeneous mixture.[46]

The net effects of the different treatments for OSPW remediation are not fully ascertained, partially because our understanding of the complete composition of the compound classes is limited. For example, most analyses of OSPW polar organics were based on negative ionization detection.[47,48] Negative and positive ionization techniques preferentially target different chemical species in petroleum samples.[49] The acidic species such as NAs (O_2 species) are readily ionized by negative-ion mode, whereas nonacid or basic species are preferentially ionized by positive-ion mode.[14,40,49] Consequently, application of a single ionization technique is less informative for full coverage of the composition of petroleum samples.[50] Comprehensive knowledge of the molecular-level composition and environmental fate of OSPW in wetland treatment is thus important for evaluating treatment efficacy as well as estimation of their potential toxicological impacts. This study reports the application of negative-ion and positive-ion APPI coupled to FT-ICR-MS to broaden the molecular characterization of wetland treatment samples previously analyzed by negative-ion ESI.

Ion formations in APPI are performed in positive or negative ionization mode. In the positive mode, basic analytes with high affinity for proton are protonated with weak acids such as formic acid (HCOOH) or acetic acid (CH_3COOH) or react with solvent or water clusters are more favorable for the formation of protonated ions ($[M + H]^+$). The acidic analytes with high affinity for positive electrons are deprotonated with weak bases such as ammonium hydroxide (NH_4OH) to produce $[M - H]^-$. Furthermore, depending on the dopant, the analytes could form either a radical molecular ion or protonated molecules. For the toluene dopant, if the analyte proton affinity is higher than the proton affinity of the benzyl radical, a protonated molecule is preferentially formed, whereas if the toluene radical cation electron affinity is higher than that of the analyte, a radical molecular ion is formed.[45,51] APPI is very useful for the characterization of slightly polar or nonpolar species and has the advantage of accessing compounds without heteroatoms such as hydrocarbons.[14] Also, the analysis of toxicologically significant compounds such as PAHs and sulfur-containing species that is not feasible with ESI is obtainable using APPI.[14,40,45,46,51]

The exhaustive characterization of the molecular composition of OSPW−NAFCs from the aerated and nonaerated wetland treatments was performed (i) to explore the fate of the NAFC species detected by the two ionization methods in the treatment systems by comparing their relative abundance and (2) to evaluate the differences between the different treatment wetlands in transforming the NAFC species detected. The CWT differs mainly in flow configuration and the presence/absence of aeration. Thus, their extent and preference to eliminate certain species based on the heteroatom, double

DOI: 10.1021/acs.energyfuels.9b00469
Energy Fuels 2019, 33, 4420−4431

bond equivalent (DBE), and carbon number will likely be different between each treatment design. The data from this study may provide more insight on the treatments at the molecular level which may enable future advancement in the improvement of the efficiency of the systems. The chemical species in the OSPW were characterized based on their relative abundances, DBE, and carbon number distributions. This approach provided qualitative information on wide ranging compound classes and a broader comparison of changes in their distributions in the aerated and nonaerated wetland treatment systems.

2. MATERIALS AND METHODS

2.1. Treatment Wetland Samples. The investigations were carried out in Contango Strategies Ltd, Saskatoon, Canada greenhouse establishment. The constructed wetlands contain a series of four identical cells operated as a closed system with the outflows redirected into the first cell of each series to prolong the hydraulic retention times (HRT). A modified schematic representation of the pilot CWT set up is shown in Figure 1. Each cell of the aerated and nonaerated treatment designs consisted of a Rubbermaid plastic bin with dimensions of 56.52 cm × 58.42 cm × 48.26 cm (length × width × depth) and filled with sand of porosity 0.26 up to 40 cm depth and 0.23 up to 30 cm depth, respectively, and both planted with sedge (*Carex aquatilis*). The OSPW used for the CWT study was collected from Shell Canada Limited's Muskeg River Mine (now operated by Canadian Natural Resources as of June 1, 2017) external tailings facility at the Athabasca oil sand region of Alberta, Canada, and brought in 1000 L plastic totes to the facility of Contango Strategies Ltd. Saskatoon, SK, Canada, on July 15, 2015. The cells were continuously fed with OSPW at a rate of 20 mL/min to achieve an HRT of 4.73 days in the aerated wetland and 5.68 days in the nonaerated system by means of FMI QG 400 pumps. The aerated wetland treatment system consists of a vertical up flow design and aerated with air stones, while the nonaerated wetland treatment system was designed with a horizontal surface flow (HSF) design. For this study, the temperature at the greenhouse facility was maintained at 22 °C from 7 am to 7 pm and at 16 °C from 7 pm to 7 am. Aqueous samples from the outflow were collected two times in a week on the same day during the entire study from October through November 2016 in each of the constructed wetlands. The samples were collected in 500 mL plastic containers and stored at 4 °C prior to analysis. The preparation of samples for analysis by the weak anion exchange solid phase extraction has been previously reported.[52,53]

2.2. Analytical Method. *2.2.1. Sample Preparation.* All samples were dissolved in equal parts tetrahydrofuran to make a final solution of 250 μg OSPW extracts/mL. As part of quality control and assurance, an instrument solvent blank was run prior to actual samples. The repeatability of mass spectra observed is estimated to be greater than 95% based on replicate injections for ∼10 percent of samples investigated.

2.2.2. 9.4 T FT-ICR MS. MS analyses were performed with a custom-built FT-ICR mass spectrometer[54] furnished with a 22 cm horizontal room temperature bore 9.4 T magnet (Oxford Corp., Oxney Mead, UK) and a modular ICR data station (Predator).[55] Ions produced at atmospheric pressure within the external APPI source (Ion Max APPI source, Thermo-Fisher Scientific, Inc., San Jose, CA, U.S.A.) go into the skimmer region at a pressure of ∼2 Torr via a heated metal capillary into an rf-only quadrupole into an octopole provided with tilted wire extraction electrodes to enhance ion extraction and transmission, where they accumulate for 50−500 ms.[56] Helium gas passed into the octopole collisionally lowers the temperature of the ions prior to conveyance through rf-only quadrupoles (total length 127 cm) with an auxiliary rf waveform provision[57] into a 7-segment open cylindrical cell.[58] Multipole ion guides were operated at 2.0 MHz and 240 V_{p-p} rf amplitude. Individual transients (150−200) of 6.1−6.8 s duration were signal-averaged. Data were collected at maximum memory depth of the data station hardware (16 million samples), apodized with a single-sided Hanning apodization, and zero-filled to 16 mega samples (16 777 216 samples or 2^{24}). An additional zero fill brings the preFT data packet to the 32 mega sample. As a result of increased complexity, broadband phase correction[59−61] was applied to mass spectra of the wetland samples in order to promote the resolution of isobaric species. For all mass spectra, the achieved mass spectral resolving power was close to the theoretical limit during accumulation to collisionally lower ion temperature before passing through a 200 cm rf-only octopole into an open cylindrical penning ion trap (10 cm i.d. × 30 cm long). Broadband frequency chirp excitation (70−700 kHz at a sweep rate of 50 Hz/μs and amplitude, V_{p-p} = 240 V) accelerated the ions to a cyclotron orbital radius that was subsequently detected by the differential current induced between two opposed electrodes of the ICR cell. Conversion of ICR frequencies to m/z was done by the quadrupolar electric trapping potential.[62,63] The internal calibration of the individual m/z spectrum was based on an abundant homologous alkylation series with members that vary in mass by an extra methylene (CH_2) unit (14.01565 Da) and confirmed by an isotopic fine structure based on the "walking" calibration equation,[58] and mass spectral peaks with a signal magnitude >6σ baseline root-mean-square (rms) noise were detected. The masses determined based on the International Union of Pure and Applied Chemistry (IUPAC) mass scale in the experiment were changed to the Kendrick mass scale[64] for easy identification of homologous series for the individual heteroatom class (i.e., species with equivalent $C_cH_hN_nO_oS_s$ composition, but vary only by their degree of alkylation).[65] For individual empirical formula, $C_cH_hN_nO_oS_s$, the heteroatom class, type (DBE = number of rings plus double bonds to carbon, DBE = $C - h/2 + n/2 + 1$),[66] and carbon number, c, were organized for subsequent generation of heteroatom class relative abundance distributions and graphical relative-abundance weighted DBE versus carbon number images. Elemental composition with the number of H unlimited, 0 < C < 100, 0 < O < 12, 0 < N < 2, 0 < S < 2, 0 < DBE < 30 were assigned. A molecular formula was considered only if the corresponding ^{13}C peak was found for hydrocarbons and ^{34}S peaks for sulfur assignments m/z were in the range 150 < m/z < 1000. PetroOrg software[67] was used for all mass spectral peak assignments and data visualization.

3. RESULTS AND DISCUSSION

3.1. Distribution of Compound Classes. Raw data from mass spectra analysis are processed using computer tools for formula attributions into classes based on Kendrick mass defect and sorted into heteroatom classes according to the number and type of heteroatom (nitrogen, oxygen, and sulfur) by measuring the exact mass.[67] Moreover, the compositions of crude oil can be conveyed by bar charts of the abundance versus heteroatom classes, and such plots provide information on the compound classes existing within a complex sample but lacking in molecular-level information.[68,69] Thus, the relative abundance plot of NAs, oxy-NAs, and heteroatom NA distributions represents a family of chemical classes with the same proportion of elements or empirical formula detected in negative-ion or positive-ion APPI-FT-ICR-MS. The relative abundance was determined as the ratio of the magnitude of individual peaks to the sum of the magnitude of all detected peaks within each mass spectrum. APPI can produce radial radical cations $[M]^{+\bullet}$ in positive mode and radial anions $[M]^{-\bullet}$ in negative mode in addition to protonated and deprotonated ions, and efficiently ionize nonpolar aromatic compounds with and without heteroatoms present. However, only low abundance of radical ions was detected in our samples. The majorities were protonated ($[M + H]^+$) and deprotonated ($[M - H]^-$) analyte ions.

3.1.1. Heteroatom Class Distribution by Negative-Ion APPI-FT-ICR MS. High-resolution negative-ion ESI orbitrap-

DOI: 10.1021/acs.energyfuels.9b00469
Energy Fuels 2019, 33, 4420−4431

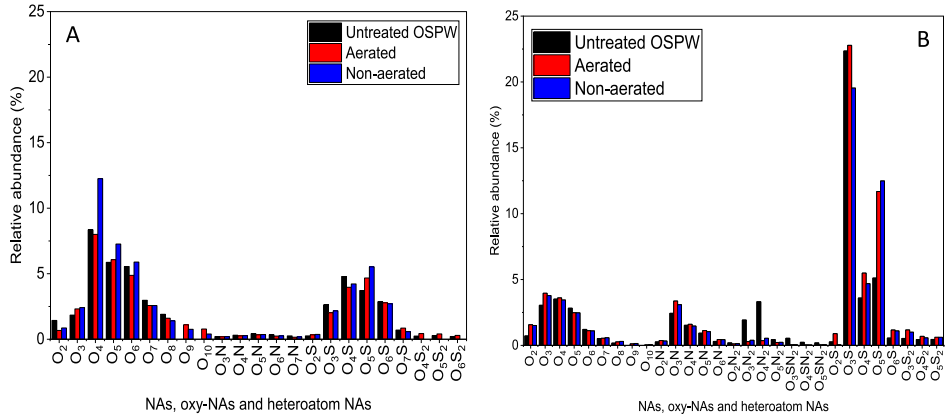

Figure 2. Relative abundances of the most abundant NAs, oxy-NAs, and heteroatom NAs determined for a single run analyzed in untreated OSPW, aerated wetland treatment, and nonaerated wetland treatment on the final day of treatment: (A) negative-ion APPI-FT-ICR-MS and (B) positive-ion APPI-FT-ICR-MS.

MS analysis of this OSPW−NAFCs in the nonaerated wetland system was already presented and discussed in our previous paper.[53] Briefly, in the negative-ion ESI-orbitrap-MS, the O_x classes have better ionization yield than in the negative-ion APPI-FT-ICR-MS used in the present study. It is presumed that this could be because of differences in ionization yield of these compound classes. Thus, analytical instruments of different design and or settings may likely generate varying yields of ionization that could have an effect on the compound class, DBE, and carbon number distributions. Furthermore, a higher number of different heteroatoms within a molecular assignment were observed in the present study by negative-ion APPI-FT-ICR-MS than in the previous study. This further reinforces the fact that the application of APPI provides broader coverage of OSPW−NAFCs. Compound class distributions derived from negative-ion APPI-FT-ICR-MS analysis of the OSPW in untreated samples and in the aerated and nonaerated wetland treatment systems are shown in Figure 2A. For untreated OSPW, O_x (x = 2−8) were the most easily ionized species and accounted for ∼20.1% of the total relative abundance. Barrow and co-workers[14] observed higher abundance of the O_x classes relative to other species in OSPW using negative-ion APPI-FT-ICR-MS. It is well known that low molecular weight carboxylic acids are more efficiently ionized in negative-ion ESI ionization modes and are disproportionally more abundant in NA samples. Therefore, the carboxylic acids will be the most representative compound classes observed in the negative ion.[51] Among the detected O_x classes, O_4 species was the most easily ionized and O_2 species was the least ionized of these species. The lower relative abundance of O_2 compared to O_4 observed by negative-ion APPI is corroborated in the literature.[40] In contrast, studies performed using Orbitrap-MS[15] and FT-ICR-MS[70] have reported a higher relative abundance of O_2 relative to O_4 species by negative-ion ESI. ESI yields quasi-molecular ions through solution phase deprotonation reactions, whereas APPI forms ions in the gas phase through three different mechanisms.[51]

Among the O_x classes in the aerated system, the O_2 class showed a decrease in relative abundance which likely corresponds to its transformation during treatment. However, the distributions of most of the species are somewhat different in the nonaerated treatment system in which the relative abundance of the O_x species (x = 3−6) noticeably increased (27.8%) compared to the untreated OSPW sample (21.6%). The increase in relative abundance of O_x species in the nonaerated system suggests that they are likely generated within the system by oxidation of the lower O_x species. Aitken et al.[71] observed that a substantial amount of organic carboxylic acids species could be formed during microbial metabolism of crude oil organic compounds under anaerobic conditions. The O_9 and O_{10} acidic species (not detected in the untreated OSPW) were detected in the aerated and nonaerated treatment wetland sample and suggest that the generation of these species may be due to the biological materials in the systems.

The O_xS_y species were the second highest in abundance in the untreated OSPW sample. The sum of the relative abundances of O_xS_y species (x = 2−7) in the untreated sample was 15.0%. Among the O_xS_y species in the untreated OSPW, O_3S, O_4S, O_5S, and O_6S were the most abundant species with relative abundances of 2.6, 4.8, 3.7, and 2.9%, respectively (Figure 2A). It is worth noting in Figure 2A that during treatment, the relative abundance of the O_xS_y (x = 3−4) decreased in the aerated and nonaerated systems, whereas a minimal increase in the relative abundance of O_xS_y (x = 5) was observed in the aerated (4.7%) and nonaerated systems (5.5%). This can be explained by the oxidation of O_3S and O_4S classes to higher O_xS classes. Some O_xS_2 were detected in the negative-ion mode at very low relative abundance (0.74% total relative abundance). The relative abundance of nitrogen-containing species observed in the negative-ion mode is the least among all the species (1.1% total relative abundance) in the sample.

3.1.2. Heteroatom Class Distribution by Positive-Ion APPI-FT-ICR-MS. The relative abundance of O_x species detected by positive-ion APPI-FT-ICR-MS can be found in Figure 2B. The relative abundance of O_x species was 12.1% before treatment. The most easily ionized O_x species observed in the untreated OSPW was the O_4 class followed by O_3 and O_5 classes. During treatment, the relative abundance of the O_3 increased minimally from 3.0% in the untreated OSPW to 4.0 and 3.8% in the aerated and nonaerated treatment systems, respectively, while the relative abundance of the O_4 did not change in both systems. An interesting observation in both wetland systems is the two-fold increase in the relative abundance of the O_2 class. This may suggest an accumulation from the molecular breakdown of the respective higher NAFC

DOI: 10.1021/acs.energyfuels.9b00469
Energy Fuels 2019, 33, 4420−4431

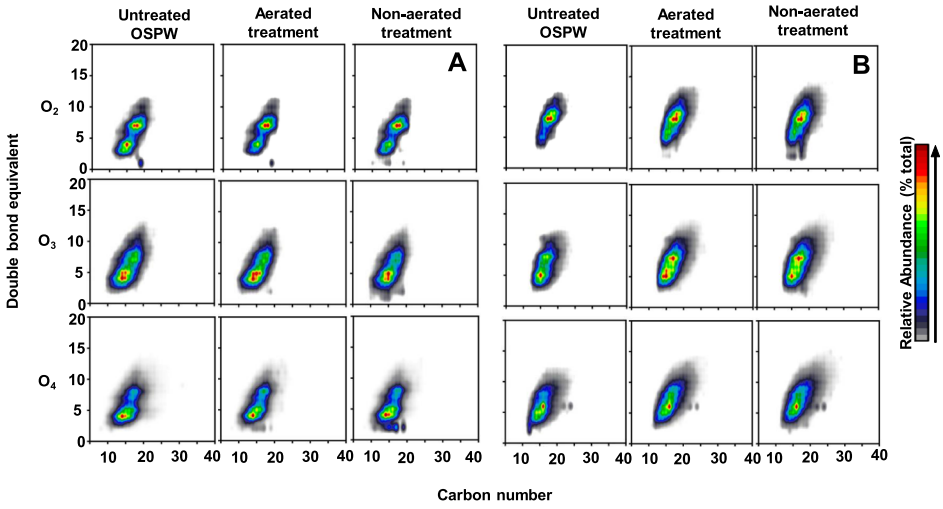

Figure 3. Isoabundance plots of DBE versus carbon number for O_x classes in untreated OSPW, aerated and nonaerated wetland treatments detected by (A) negative-ion APPI-FT-ICR-MS and (B) positive-ion APPI-FT-ICR-MS (right). The color intensity on the scale depicts the relative abundance of ions within the compound class.

species or NAFC-containing organic materials in the wetland systems.

The O_xS_y were the most dominant species detected in positive-ion APPI prior to treatment. The distribution of these species was different in both ionization modes (Figure 2). For example, the most prevalent O_xS_y species in positive-APPI were O_3S (22.4%), followed by O_5S (5.1%) and O_4S (3.6%). The sum of the relative abundance of O_xS_y species in the untreated sample increased from 33.3 to 44.5 and 40.0% in the aerated and nonaerated systems, respectively. The relative abundance of O_3S species decreased to 19.5% in the nonaerated system and does not change significantly in the aerated system (22.8%). This result suggests that environmental conditions are likely more favorable for the transformation of O_3S class in the nonaerated wetland than the aerated wetland and indicates that the degradation characteristics of the two treatment systems are different. The O_3S species remained relatively the highest abundant O_xS_y compound detected in positive-ion APPI. The relative abundance of O_4S, O_5S, and O_6S classes in the treatment wetlands (i.e., 5.5, 11.75, and 1.2%, respectively in aerated wetland and 4.5, 12.5, and 1.1%, respectively, in nonaerated wetland) was higher relative to the untreated sample (i.e., 3.6, 5.15 and 0.6% respectively) which may be due to oxidation of the sulfur-containing compounds in OSPW. OSPW is composed of sulfur-containing compounds that are readily oxidized such as the sulfurs that have nonbonding electrons and exist in low oxidation states (i.e., sulfurs present in thiophenic compounds and sulfides found in sulfur-containing carboxylic acid).[70] Nitrogen-containing species (O_xN_y) were detected by positive-ion APPI. The presence of the O_xN_2 species in OSPW formed from the dimerization of the O_xN classes was earlier suggested.[70,72] Also detected in the positive-ion APPI is the $O_xS_{y1}N_{y2}$ class. However, the relative abundances of these species in the untreated OSPW were very low (0.96% total relative abundance).

Overall, a comparison of the negative-ion APPI and positive-ion APPI heteroatom class plots indicate differences in the relative abundances among the compound classes in the aerated and nonaerated wetland treatments. The trend discerned in the distribution of most compound classes from the aerated and nonaerated treatment systems was different for both ionization techniques employed. For example, the relative abundance of the O_2 classes in the aerated and nonaerated systems in negative-ion APPI showed reduction relative to the untreated sample, while for the positive ion, the relative abundance of this species increased. Furthermore, between the aerated and nonaerated wetland treatments, some differences in relative abundances were observed within the compound classes for every ionization mode. These differences could be due to the design and relevant operational conditions of each wetland system. Recently, Li et al.[29] reported that the extent of removal of organic contaminants in constructed wetland is dependent on the design and operational conditions.

3.2. DBE Versus Carbon Number Analysis. DBE versus carbon number iso-abundance plots of FT-ICR-MS data is an excellent tool for understanding the molecular composition of complex samples. Additionally, speciation based on DBE versus carbon number can provide compositional information on the chemical species[73] and is often applied in the analysis of high-resolution mass spectra data derived from crude oil samples.[74,75] The responses of the compound classes detected in petroleum samples such as crude oil samples are usually displayed as plots of DBE versus relative abundance versus carbon number to provide proper visualization of the qualitative differences between samples as well as the most representative species within a heteroatom class.[68,73] DBE versus carbon number distributions of the species of the untreated OSPW and the aerated and nonaerated wetland systems on the final day of treatment are discussed in this section and are mainly focused on O_x (x = 2−4), O_xS (x = 2−4) and O_xN (x = 3−5) classes. Effect directed analysis using ultrahigh resolution MS associated acute toxicity of OSPW mainly to classical NAs (O_2^-), oxy-NAs, and basic chemical species containing sulfur and nitrogen.[18,20] In addition to O_2^- species, the compound classes O_2S^-, O_2^+, O_2S^+, O_3^-, O_4^-, and O_3S^- contribute to acute toxicity of OSPW.[19,20,76] Moreover, the ratios of the abundances of O_4S^- together with O_2S^- and O_3S^- ($O_2S/O_3S/O_4S$) and O_2/O_4 ratios have the potential for use in environmental forensics to distinguish OSPW sources and to monitor treatment performance by developing ratios to evaluate the extent of biodegradation.[77,78] However, the O_xN

DOI: 10.1021/acs.energyfuels.9b00469
Energy Fuels 2019, 33, 4420−4431

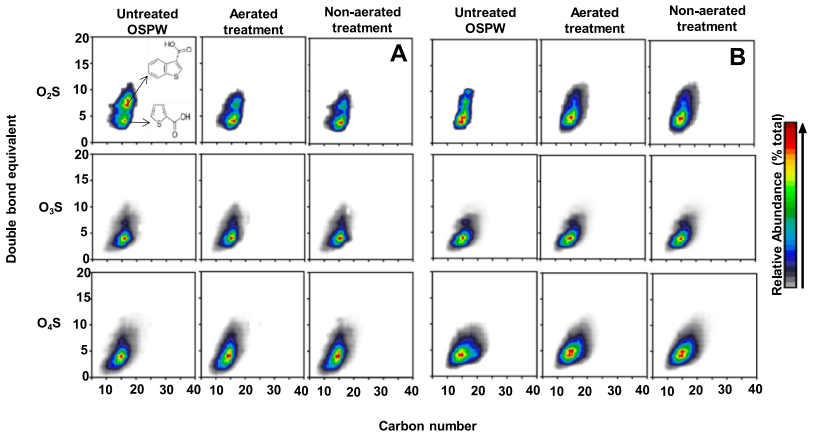

Figure 4. Isoabundance plots of DBE versus carbon number for O_xS classes in untreated OSPW, aerated, and nonaerated wetland treatments detected by (A) negative-ion APPI-FT-ICR-MS and (B) positive-ion APPI-FT-ICR-MS (right). The color intensity on the scale depicts the relative abundance of ions within the compound class.

(x = 3−5) species were chosen because they are the most abundant compounds in the positive-ion APPI. Therefore, the selection of these species was based on these criteria in order to evaluate their fate and behavior together with those of their corresponding counterpart species of opposite polarity in these wetland systems.

3.2.1. Oxygen-Containing Species. The plot of the DBE as a function of carbon number in negative-ion APPI-FT-ICR-MS for O_x (x = 2−4) that mainly represent NAs and oxygenated NAs is shown in Figure 3A. The O_2 exhibits two sets of distinct most intense relative abundances for untreated OSPW at lower DBE = 3−4 and C13−17 (77.6%) and at higher DBE = 7−8 and C17−20 (76.8%). This observation is in agreement with the negative-ion ESI data previously reported for OSPW analysis.[52,79] An interesting comparison with our past study by negative-ion ESI-HRMS showed that the highest intensity for the O_2 class is also centered on DBE = 3−4. However, with the APPI data, higher distribution of DBE was observed (DBE = 2−12) than in the previous study with ESI data (DBE = 2−8).[53] This difference in distribution is likely because chemical species with higher DBE values are more easily ionized by APPI mode. Compound classes with DBE = 3−4 are likely nonaromatic species, or they could be six-membered ring species containing double hydroxyl groups and DBE = 7−8 species are probably aromatic compounds.[79] It could be noticed that the relative abundance of the species with DBE = 3−4 decreased during treatments. DBE changes with regard to the relative abundance of the species with highest ionization yield (DBE = 3−4) was observed in the aerated wetland (25.4%) and the nonaerated wetland (23.2%). In addition, the DBE changes observed for DBE = 7−8 and C17−20 were 42.9 and 32.9% for aerated and nonaerated treatment systems, respectively. In both treatment systems, the species with lower DBE values decreased more than those with higher DBE. Previous studies hold the view that O_2−NAs with higher aromaticity are more recalcitrant to biodegradation than the less aromatic congeners.[25] However, the decrease in the relative abundance of this species was more evident in the nonaerated system and demonstrates that its efficiency for transformation of the more aromatic species may be higher compared to the aerated wetland system. The DBE versus carbon number distribution of O_3 class showed significant dominance at DBE = 3−6 and C13−17 and that of the O_4 class has the highest relative abundance at 3−5 and C12−18. However, these species showed no change in their relative abundances which may suggest that they are generated during treatment in both systems. In addition, a recent study reported that aerobic and anaerobic biodegradation of crude oil generates O_3 (hydroxyl fatty acids) and O_4 (dibasic fatty acids) classes.[80]

In the positive-ion APPI data Figure 3B, O_2 compounds with DBE = 8−9 and C16−19 (15.0%) were predominant in the untreated sample. A similar increase in relative abundance of these DBE species to 27.8 and 27.5% was detected in aerated and nonaerated systems, respectively. The O_3 class showed its highest relative abundance in the untreated OSPW at DBE = 4−5 and C14−16 (43.8%). Also, there is high relative abundance of the chemical class with DBE = 7−9 and C15−17 (51.1%) in this sample. The relative abundance of these NA class decreased less significantly in the nonaerated system (42.6%), while better enhancement was found in the aerated wetland (48.3%). However, enhancement in the intensity of the relative abundance of these species of DBE = 7−9 and C15−17 was discerned in both treatment systems (76.5% in the aerated wetland and 78.6% in the nonaerated wetland) and may indicate oxidation of some species to form high DBE compounds. For the O_4 class, species with DBE = 5−7 and C14−16 were most prevalent in relative abundance. Relatively, there was no apparent change in the DBE and carbon number distributions for these compounds in the aerated and nonaerated treatments.

The O_2 species obtained by negative-ion and positive-ion APPI revealed a similar trend and differences in the relative abundance of DBE and carbon number distributions between the aerated and nonaerated treatment systems. Additionally, DBE and carbon number distribution for each O_x compound class detected by negative-ion APPI were similar within each sample but different compared to the data obtained by positive-ion APPI and further highlight the need for complimentary ionization techniques for the detailed characterization of OSPW compounds. Pereira et al.[47] reported the distinction between O_2 species with same empirical formula detected by the negative-ion mode (NAs) and positive-ion mode (non-acids or polar neutral species). The O_2 species detected in the positive-ion mode were tentatively assigned as ketohydroxy, diketo or dihydroxy compounds.[47,81]

3.2.2. Sulfur-Containing Species. To illustrate the molecular composition for sulfur-containing classes (O_2S, O_3S, and

DOI: 10.1021/acs.energyfuels.9b00469
Energy Fuels 2019, 33, 4420−4431

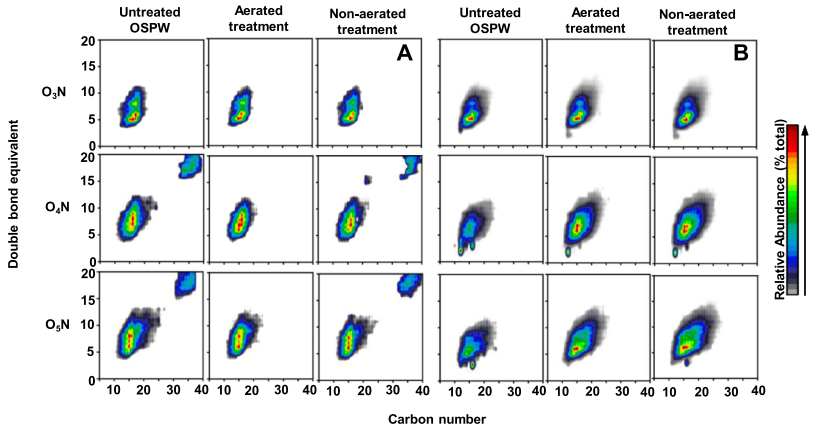

Figure 5. Isoabundance plots of DBE versus carbon number for O_xN classes in untreated OSPW, aerated, and nonaerated treatment wetlands detected by (A) negative-ion APPI-FT-ICR-MS and (B) positive-ion APPI-FT-ICR-MS (right). The color intensity on the scale depicts the relative abundance of ions within the compound class.

O_4S) from the negative-ion APPI-FT-ICR-MS analysis, isoabundance plots of DBE as a function of carbon number are shown in Figure 4A. In the untreated OSPW, the O_2S class has two sets of distinct regions of highest relative intensities (abundance) at DBE = 4−5/C14−17 (12.7%) and DBE = 7−9/C14−17 (18.5%), indicating the presence of both low and higher aromatic species. This finding is consistent with the bimodal distribution of O_2S species reported previously in untreated Athabasca oil sand bitumen by negative-ion ESI-FT-ICR-MS.[82,83] It is suggested that the high relative abundance of DBE = 4 and DBE = 7 species represents two stable core structures in this chemical class; species with DBE = 4 are mainly thiophenic ring-containing carboxylic acids and the more aromatic species with DBE = 7 are mainly benzothiophenic ring components that contain a carboxylic acid group.[83] For this ionization method, two conspicuous changes were recognized in the aerated and nonaerated treatment wetlands. First, the two treatment wetlands displayed selective transformation of the higher DBE = 7−9 (16.4 and 13.0% in aerated and nonaerated systems, respectively). Prior to the wetland treatments, the species with DBE = 4−5 had lower relative abundance than species with DBE = 7−9. Second, in the wetlands, a reversed trend was notable with the enhancement in the relative abundance of the species with values of DBE = 4−5 (18.9 and 23.7% in aerated and nonaerated systems, respectively). It is likely that the transformation of larger DBE species in the treatment systems contributed to the increased enhancement of the lower DBE compounds. Previous studies have shown that microbes can transform some precursor OSPW compounds with more rings to species with fewer rings.[84,85] The O_3S class spread from DBE = 3−10 and C10−20, and the dominant species detected were at DBE = 4−5 and C14−17 in the untreated sample. However, during treatment in the two wetland systems, no significant change was noticed in the relative abundance of these species. The O_4S class identified in the untreated OSPW had values of DBE = 2−10 and C10−20. The highest intensity among this class in the untreated sample had DBE = 3−5 and C14−16. This result obtained for the negative-ion APPI-FT-ICR-MS analysis with species of highest abundance at DBE = 3−5 for the untreated OSPW sample is comparable to the range of DBE (DBE = 2−5) for the O_4S species as determined by negative-ion ESI-FT-ICR-MS in our previous study.[52] Moreover, within the two treatment wetlands, the intensities of DBE distribution of the dominant species increased compared to the untreated OSPW, indicating that some compounds were enriched.

Figure 4B shows the DBE versus carbon number distribution of O_xS obtained by positive-ion APPI-FT-ICR-MS. The data for O_2S in untreated OSPW show distribution mainly from DBE = 3−10 and the carbon number range of 12−19 and also showed that species with DBE = 4−5 and C14−16 have the highest relative abundance. There was no significant change in relative abundance of DBE and carbon numbers observed of these species. For the O_4S class, an area of highest relative abundance was observed at DBE = 4−6 and C13−16. In both treatment systems, these species were enriched.

In summary, our data suggest not only that treatment in the aerated and nonaerated wetlands changed the DBE and carbon number profile of some O_xS species, but also that the degree of their transformation was comparable. Also, the distributions of the O_2S class in both negative and positive ionization modes differ remarkably. For example, the O_2S detected by positive-ion APPI has one region of highest relative abundance at lower DBE = 4−5 unlike negative-ion APPI O_2S ions with two areas of highest relative abundance (DBE = 4−5 and 7−9). Therefore, the O_2S class observed by negative-ion APPI contains more aromatic species than the same compound class by positive-ion APPI. Barrow et al.[86] showed that O_2S in OSPW observed by the negative-ion mode and those detected by positive-ion mode are distinct chemical species. The abundance of O_4S species detected by both ionization techniques increased in the two treatment systems. The O_xS classes are not easily ionized by both negative-ion and positive-ion modes because of the complexity of these classes of compounds that may have different functional groups such as sulfoxides and acidic sulfur compounds.[47] This complex feature of the O_xS classes may be the reason for the recalcitrance observed for the O_3S and O_4S classes in both wetland systems.

3.2.3. Nitrogen-Containing Species. The iso-abundance plot of DBE versus carbon number of the most easily ionized O_xN classes (x = 3−5) as observed by negative-ion APPI-FT-ICR-MS is displayed in Figure 5A. The highest relative abundance of the O_3N class was at DBE = 4−6 and C14−18 (15.4%). Low relative abundance was also observed for these species at DBE = 8−9 and C15−17 (9.1%), indicating the presence of more aromatic species. In the aerated wetland systems, relative abundances of the species at DBE = 4−6

DOI: 10.1021/acs.energyfuels.9b00469
Energy Fuels 2019, 33, 4420−4431

showed minimal change (13.6%) compared to the nonaerated wetland (10.9%). Also, compounds with higher DBE = 8−9 decreased by 8.1% in the aerated wetland compared to 6.1% in the nonaerated system wetland. This might reflect a higher preference for the transformation of these species in the nonaerated system. Before the commencement of OSPW treatment, the O_4N compound class showed apparently two structural features at DBE = 4−12 and C11−23 (with highest relative abundance at DBE = 6−9/C15−17) and compounds of lesser intensity at higher DBE ≥ 16 and C ≥ 30. The O_5N class showed similar characteristics at DBE = 4−13 and C11−26 (with highest relative abundance at DBE = 6−9/C11−26) and compounds of lesser intensity at higher DBE ≥ 16 and C ≥ 30. This result strongly suggests that the O_xN (x = 4−5) with DBE ≥ 16 contain highly aromatic species with multirings. These species are likely nitrogen-containing structures that are present in petroleum samples.[87] Decrease in the relative abundance of the O_4N compounds with DBE ≥ 16 was noticeable in the nonaerated treatment system. However, the O_4N and O_5N compounds with higher DBE and carbon numbers were absent in the negative-ion APPI data for the aerated wetland. Considering the disappearance of these compounds when compared with the nonaerated wetland, it could be inferred that they are preferentially transformed in the aerated system. The presence or absence of aeration generates several micro-environments within constructed wetland, which can support different microbial populations, and diverse microbial populations have unique preferences for the degradation of organic contaminants.[88] However, determination of the microbial populations present in each wetland design during the treatment process was not evaluated in this study. Bedessem et al.[89] employed pilot-scale constructed wetlands ran in parallel in vertical upflow or HSF regimes with the presence or absence of aeration for the treatment of oilfield impacted groundwater. They observed that the extent of removal of petroleum organic contaminants was affected by the presence or absence of aeration. Furthermore, the species with less cyclicity and alkyl chain showed more resistance to transformation and imply that both treatment wetlands preferentially transform higher ring structures and alkyl chains than the species with fewer rings and alkyl chains. For the O_5N class (DBE = 4−13 range and abundance-weighted average of 24 carbon), the abundance-weighted average of carbons decreased to 22 and 23 carbons in the aerated and nonaerated systems, respectively (i.e., a few carbons less than that in the untreated OSPW sample). This indicates that for these species, the transformation of the alkyl chains is likely more favorable.

In Figure 5B, the isoabundance plot of DBE versus carbon number for the O_xN (x = 3−5) obtained using positive-ion APPI is shown. The species with highest relative abundance were observed at DBE = 4−6 and C14−16. There was no significant change in the DBE and carbon numbers for O_3N classes detected by positive-ion APPI in both the aerated and non-aerated wetland treatments compared to the untreated sample. It appears that these species are more resistant to transformation. In the untreated OSPW, O_4N has the DBE ranges of 2−9 and C12−19 and O_5N has the ranges of DBE = 3−10 and C11−20. However, in the treatment wetland systems for O_4N and O_5N classes, the relative abundance of DBE and carbon number range of these species were enhanced in the aerated system and in the nonaerated system. An increment in DBE is probably due to the inclusion of cyclic structures or double bonds to a carbon atom.[40] Moreover, the relative abundance of O_4N species with DBE = 5−8 and C13−17 increased from 37.4 to 44.9 and 44.2% in aerated and nonaerated wetlands, respectively, and that of O_5N species with DBE = 5−7 and C13−17 increased from 20.0 to 24.5 and 24.1% in aerated and nonaerated wetlands, respectively. The enrichment of the O_xN (x = 4−5) compounds suggest that they may be generated from the transformation of other species during treatments or from other N-containing compounds that have experienced ring opening of the hydroxyl dibenzocarbazoles due to the addition of the carboxyl functional group.[90]

DBE versus carbon number parameters were used to assess composition and variability of OSPW compound classes. Despite the differences in the data obtained by negative-ion APPI for the O_xN compound classes between aerated and nonaerated systems, some similarities in the data by positive-ion APPI were obvious for these compound classes. It is believed that the differences between the treatment wetland systems were caused by their different configurations mainly in the flow path and with or without aeration. As previously stated, selectivity and extent of transformation of some species detected by both ionization modes thus depend on the design of the treatment system.

3.3. O_2−NA Transformation Rates. The natural logarithm of the relative abundance of the total O_2−NAs detected by negative-ion and positive-ion APPI was plotted against time (Figure 6) to determine the kinetics of their transformation.

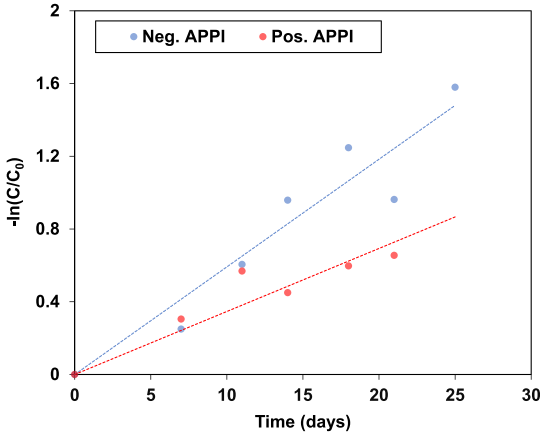

Figure 6. Transformation rate of total O_2−NAs in the aerated treatment wetland monitored by negative-ion and positive-ion APPI-FT-ICR-MS.

The rate coefficient (k) for NAs from the techniques were obtained from line of best fit for the first-order transformation of NAs, indicating trends that fit the measured abundance over time using $kt = -\ln([C])/([C_0])$, where C is the total abundance at time t; C_0 is the initial abundance at time 0; k is the transformation rate coefficient (slope), and t is time (days). The decrease in abundance for a given time t was defined as changes in the abundance of the species (C) relative to the initial abundance (C_0) according to procedure previously reported by Toor et al.[91] but using total abundance of O_2−NAs rather than fractional abundance of the species. The standard deviation of the slope reported in this work was estimated from the regression line. The correlation coefficients (R^2) for the negative-ion and positive ion APPI are 0.9108 and 0.8740, respectively, suggesting a first-order kinetics with

DOI: 10.1021/acs.energyfuels.9b00469
Energy Fuels 2019, 33, 4420−4431

positive correlations for the decrease in abundance over time. It can be noted from the plot that the rate of transformation was more rapid in the negative-ion APPI for O_2^- species (0.06176 ± 0.00864 d^{-1}) than for O_2^+ species detected by the positive-ion APPI (0.02997 ± 0.00569 d^{-1}). This reinforces the fact that different populations of component ionization efficiency vary with ionization methods and yield different rates of transformation. Thus, the kinetic data suggest that the rate of transformation was controlled by the chemical composition and provided information on the magnitude of their transformation which may determine if measures are required to enhance the transformation rate of the compounds in the treatment systems. The intent of this work was not to determine or discuss the rates of transformation of total classical NA but rather to further highlight that the data obtained by negative-ion and positive-ion APPI significantly differ and both ionization modes are important for a more exhaustive elucidation of the fate of OSPW components in the treatment wetlands at the molecular-level. In our previous study by negative-ion ESI Orbitrap-MS, the rates of NA components were reported for the nonaerated wetland. The rates were recorded between 0.0464 and 0.0574 d^{-1} for DBE and between 0.0308 and 0.0743 d^{-1} for the carbon number.[52] In comparison, comparable magnitude was observed between the rates of the negative-ion APPI and that of the individual components obtained previously with negative-ion ESI. While the data for this study indicated the effect of chemical composition has on the transformation rates, it does not adequately characterize the fate of NAs in the treatment systems. The transformation rate is useful for determining the remediation time span.

4. CONCLUSIONS

OSPW from aerated and nonaerated CWTs were analyzed using negative-ion and positive-ion APPI-FT-ICR-MS. The compound classes detected by the two ionization techniques were categorized based on DBE and carbon number. Overall, transformation of most NAFC species was achieved in both the aerated and nonaerated wetland treatment systems. Information obtained from the DBE versus carbon number analysis revealed different levels of transformation of the compound classes as indicators of their susceptibility to transformation. The extent of the changes in distribution with regards to the heteroatom class, DBE, and carbon number is dependent on the type of wetland treatment system. Furthermore, the use of negative-ion and positive-ion APPI-FT-ICR-MS provided complementary data to previous analysis by negative-ion ESI and enhanced the molecular identification of the organic compound classes investigated. The OSPW−NAFCs observed by these two ionization methods were compositionally different with unique distribution of DBE and carbon numbers. This compositional difference may probably cause contrasting influence on the fate of these compounds and environmental toxicity. Furthermore, for comprehensive information on NAFC species present in OSPW, the use of one method of ionization for the characterization of OSPW−NAFCs may result in incomplete evaluation because some NAFCs may not ionize at all.

AUTHOR INFORMATION

Corresponding Author

*E-mail: dena.mcmartin@usask.ca.

ORCID

Amy M. McKenna: 0000-0001-7213-521X

Dena W. McMartin: 0000-0002-0824-0565

Notes

The authors declare no competing financial interest.

ACKNOWLEDGMENTS

This research was financially supported by the Program of Energy Research and Development (PERD) and the University of Regina graduate student funding. We also appreciated the help rendered by Rachel Martz in routine sample collection and to Dr. Monique Simair and Dr. Vanessa Friesen for the experimental design and setup of the CWT systems. A portion of this work was performed at the National High Magnetic Field Laboratory at Florida State University, which is supported by the National Science Foundation Division of Materials Research through DMR 11-57490 and DMR 16-44779, and the State of Florida.

REFERENCES

(1) Whitby, C. Microbial Naphthenic Acid Degradation. *Adv. Appl. Microbiol.* **2010**, *70*, 93−125.

(2) Czarnecki, J.; Radoev, B.; Schramm, L. L.; Slavchev, R. On the nature of Athabasca oil sands. *Adv. Colloid Interface Sci.* **2005**, *114-115*, 53−60.

(3) Noah, M.; Poetz, S.; Vieth-Hillebrand, A.; Wilkes, H. Detection of Residual Oil-Sand-Derived Organic Material in Developing Soils of Reclamation Sites by Ultra-High-Resolution Mass Spectrometry. *Environ. Sci. Technol.* **2015**, *49*, 6466−6473.

(4) Giesy, J. P.; Anderson, J. C.; Wiseman, S. B. Alberta oil sands development. *Proc. Natl. Acad. Sci. U.S.A.* **2010**, *107*, 951−952.

(5) El-Din, M. G.; Fu, H.; Wang, N.; Chelme-Ayala, P.; Perez-Estrada, L.; Drzewicz, P.; Martin, J. W.; Zubot, W.; Smith, D. W. Naphthenic acids speciation and removal during petroleum-coke adsorption and ozonation of oil sands process-affected water. *Sci. Total Environ.* **2011**, *409*, 5119−5125.

(6) Demeter, M. A.; Lemire, J. A.; Yue, G.; Ceri, H.; Turner, R. J. Culturing oil sands microbes as mixed species communities enhances ex situ model naphthenic acid degradation. *Front. Microbiol.* **2015**, *6*, 936.

(7) Mahaffey, A.; Dubé, M. Review of the composition and toxicity of oil sands process-affected water. *Environ. Rev.* **2017**, *25*, 97−114.

(8) Hughes, S. A.; Mahaffey, A.; Shore, B.; Baker, J.; Kilgour, B.; Brown, C.; Peru, K. M.; Headley, J. V.; Bailey, H. C. Using ultrahigh-resolution mass spectrometry and toxicity identification techniques to characterize the toxicity of oil sands process-affected water: the case for classical naphthenic acids. *Environ. Toxicol. Chem.* **2017**, *36*, 3148−3157.

(9) Li, C.; Fu, L.; Stafford, J.; Belosevic, M.; Gamal El-Din, M. The toxicity of oil sands process-affected water (OSPW): A critical review. *Sci. Total Environ.* **2017**, *601-602*, 1785−1802.

(10) Li, C.; Fu, L.; Stafford, J.; Belosevic, M.; Gamal El-Din, M. The toxicity of oil sands process-affected water (OSPW): A critical review. *Sci. Total Environ.* **2017**, *601-602*, 1785−1802.

(11) Allen, E. W. Process water treatment in Canada's oil sands industry: I. Target pollutants and treatment objectives. *J. Environ. Eng. Sci.* **2008**, *7*, 123−138.

(12) McQueen, A. D.; Kinley, C. M.; Hendrikse, M.; Gaspari, D. P.; Calomeni, A. J.; Iwinski, K. J.; Castle, J. W.; Haakensen, M. C.; Peru, K. M.; Headley, J. V.; Rodgers, J. H., Jr A risk-based approach for identifying constituents of concern in oil sands process-affected water from the Athabasca Oil Sands region. *Chemosphere* **2017**, *173*, 340−350.

(13) McQueen, A. D.; Hendrikse, M.; Gaspari, D. P.; Kinley, C. M.; Rodgers, J. H., Jr.; Castle, J. W. Performance of a hybrid pilot-scale

DOI: 10.1021/acs.energyfuels.9b00469
Energy Fuels 2019, 33, 4420−4431

constructed wetland system for treating oil sands process-affected water from the Athabasca oil sands. *Ecol. Eng.* **2017**, *102*, 152−165.
(14) Barrow, M. P.; Witt, M.; Headley, J. V.; Peru, K. M. Athabasca oil sands process water: Characterization by atmospheric pressure photoionization and electrospray ionization Fourier transform ion cyclotron resonance mass spectrometry. *Anal. Chem.* **2010**, *82*, 3727−3735.
(15) Zhang, K.; Pereira, A. S.; Martin, J. W. Estimates of Octanol-Water Partitioning for Thousands of Dissolved Organic Species in Oil Sands Process-Affected Water. *Environ. Sci. Technol.* **2015**, *49*, 8907−8913.
(16) Headley, J. V.; Peru, K. M.; Fahlman, B.; Colodey, A.; McMartin, D. W. Selective solvent extraction and characterization of the acid extractable fraction of Athabasca oils sands process waters by Orbitrap mass spectrometry. *Int. J. Mass Spectrom.* **2013**, *345-347*, 104−108.
(17) Hughes, S. A.; Huang, R.; Mahaffey, A.; Chelme-Ayala, P.; Klamerth, N.; Meshref, M. N. A.; Ibrahim, M. D.; Brown, C.; Peru, K. M.; Headley, J. V.; Gamal El-Din, M. Comparison of methods for determination of total oil sands-derived naphthenic acids in water samples. *Chemosphere* **2017**, *187*, 376−384.
(18) Morandi, G. D.; Wiseman, S. B.; Pereira, A.; Mankidy, R.; Gault, I. G. M.; Martin, J. W.; Giesy, J. P. Effects-directed analysis of dissolved organic compounds in oil sands process-affected water. *Environ. Sci. Technol.* **2015**, *49*, 12395−12404.
(19) Quesnel, D. M.; Oldenburg, T. B. P.; Larter, S. R.; Gieg, L. M.; Chua, G. Biostimulation of oil sands process-affected water with phosphate yields removal of sulfur-containing organics and detoxification. *Environ. Sci. Technol.* **2015**, *49*, 13012−13020.
(20) Morandi, G. D.; Zhang, K.; Wiseman, S. B.; Pereira, A. D. S.; Martin, J. W.; Giesy, J. P. Effect of lipid partitioning on predictions of acute toxicity of oil sands process affected water to embryos of fathead minnow (Pimephales promelas). *Environ. Sci. Technol.* **2016**, *50*, 8858−8866.
(21) Alharbi, H. A.; Saunders, D. M. V.; Al-Mousa, A.; Alcorn, J.; Pereira, A. S.; Martin, J. W.; Giesy, J. P.; Wiseman, S. B. Inhibition of ABC transport proteins by oil sands process affected water. *Aquat. Toxicol.* **2016**, *170*, 81−88.
(22) McMartin, D. W.; Headley, J. V.; Friesen, D. A.; Peru, K. M.; Gillies, J. A. Photolysis of Naphthenic Acids in Natural Surface Water. *J. Environ. Sci. Health, Part A: Toxic/Hazard. Subst. Environ. Eng.* **2004**, *39*, 1361−1383.
(23) Janfada, A.; Headley, J. V.; Peru, K. M.; Barbour, S. L. A laboratory evaluation of the sorption of oil sands naphthenic acids on organic rich soils. *J. Environ. Sci. Health Pt. A-Toxic/Hazard. Subs. Environ. Eng.* **2006**, *41*, 985−997.
(24) Scott, A. C.; Zubot, W.; MacKinnon, M. D.; Smith, D. W.; Fedorak, P. M. Ozonation of oil sands process water removes naphthenic acids and toxicity. *Chemosphere* **2008**, *71*, 156−160.
(25) Martin, J. W.; Barri, T.; Han, X.; Fedorak, P. M.; El-Din, M. G.; Perez, L.; Scott, A. C.; Jiang, J. T. Ozonation of Oil Sands Process-Affected Water Accelerates Microbial Bioremediation. *Environ. Sci. Technol.* **2010**, *44*, 8350−8356.
(26) Mishra, S.; Meda, V.; Dalai, A. K.; McMartin, D. W.; Headley, J. V.; Peru, K. M. Photocatalysis of naphthenic acids in water. *J. Water Resour. Prot.* **2010**, *02*, 644−650.
(27) Choi, J.; Hwang, G.; Gamal El-Din, M.; Liu, Y. Effect of reactor configuration and microbial characteristics on biofilm reactors for oil sands process-affected water treatment. *Int. Biodeterior. Biodegrad.* **2014**, *89*, 74−81.
(28) Sun, N.; Chelme-Ayala, P.; Klamerth, N.; McPhedran, K. N.; Islam, M. S.; Perez-Estrada, L.; Drzewicz, P.; Blunt, B. J.; Reichert, M.; Hagen, M.; Tierney, K. B.; Belosevic, M.; Gamal El-Din, M. Advanced analytical mass spectrometric techniques and bioassays to characterize untreated and ozonated oil sands process-affected water. *Environ. Sci. Technol.* **2014**, *48*, 11090−11099.
(29) Li, Y.; Zhu, G.; Ng, W. J.; Tan, S. K. A review on removing pharmaceutical contaminants from wastewater by constructed wetlands: design, performance and mechanism. *Sci. Total Environ.* **2014**, *468-469*, 908−932.
(30) Rodgers, J. H., Jr.; Castle, J. W. Constructed wetland systems for efficient and effective treatment of contaminated waters for reuse. *Environ. Geosci.* **2008**, *15*, 1−8.
(31) Haakensen, M.; Pittet, V.; Spacil, M. M.; Castle, J. W.; Rodgers, J. H., Jr. Key aspects for successful design and implementation of passive water treatment systems. *J. Environ. Solut. Oil Gas Min.* **2015**, *1*, 59−81.
(32) García, J.; Rousseau, D. P. L.; Morató, J.; Lesage, E.; Matamoros, V.; Bayona, J. M. Contaminant removal processes in subsurface-flow constructed wetlands: a review. *Crit. Rev. Environ. Sci. Technol.* **2010**, *40*, 561−661.
(33) Pham, M. P. T.; Castle, J. W.; Rodgers, J. H., Jr. Biogeochemical process approach to the design and construction of a pilot-scale wetland treatment system for an oil field-produced water. *Environ. Geosci.* **2011**, *18*, 157−168.
(34) Cooper, P. A Review of the Design and Performance of Vertical-flow and Hybrid Reed Bed Treatment Systems. *Water Sci. Technol.* **1999**, *40*, 1−9.
(35) Dong, H.; Qiang, Z.; Li, T.; Jin, H.; Chen, W. Effect of artificial aeration on the performance of vertical-flow constructed wetland treating heavily polluted river water. *J. Environ. Sci.* **2012**, *24*, 596−601.
(36) Foladori, P.; Ruaben, J.; Ortigara, A. R. C. Recirculation or artificial aeration in vertical flow constructed wetlands: A comparative study for treating high load wastewater. *Bioresour. Technol.* **2013**, *149*, 398−405.
(37) Pomerantz, A. E.; Mullins, O. C.; Paul, G.; Ruzicka, J.; Sanders, M. Orbitrap Mass Spectrometry: A Proposal for Routine Analysis of Nonvolatile Components of Petroleum. *Energy Fuels* **2011**, *25*, 3077−3082.
(38) McKenna, A. M.; Nelson, R. K.; Reddy, C. M.; Savory, J. J.; Kaiser, N. K.; Fitzsimmons, J. E.; Marshall, A. G.; Rodgers, R. P. Expansion of the analytical window for oil spill characterization by ultrahigh resolution mass spectrometry: beyond gas chromatography. *Environ. Sci. Technol.* **2013**, *47*, 7530−7539.
(39) Headley, J. V.; Peru, K. M.; Armstrong, S. A.; Han, X.; Martin, J. W.; Mapolelo, M. M.; Smith, D. F.; Rogers, R. P.; Marshall, A. G. Aquatic plant-derived changes in oil sands naphthenic acid signatures determined by low-, high- and ultrahigh-resolution mass spectrometry. *Rapid Commun. Mass Spectrom.* **2009**, *23*, 515−522.
(40) Barrow, M. P.; Peru, K. M.; Fahlman, B.; Hewitt, L. M.; Frank, R. A.; Headley, J. V. Beyond Naphthenic Acids: Environmental Screening of Water from Natural Sources and the Athabasca Oil Sands Industry Using Atmospheric Pressure Photoionization Fourier Transform Ion Cyclotron Resonance Mass Spectrometry. *J. Am. Soc. Mass Spectrom.* **2015**, *26*, 1508−1521.
(41) Marshall, A. G.; Rodgers, R. P. Petroleomics: Chemistry of the underworld. *Proc. Natl. Acad. Sci. U.S.A.* **2008**, *105*, 18090−18095.
(42) Bowman, D. T.; Jobst, K. J.; Ortiz, X.; Reiner, E. J.; Warren, L. A.; McCarry, B. E.; Slater, G. F. Improved coverage of naphthenic acid fraction compounds by comprehensive two-dimensional gas chromatography coupled with high resolution mass spectrometry. *J. Chromatogr. A* **2018**, *1536*, 88−95.
(43) Barrow, M. P.; Headley, J. V.; Peru, K. M.; Derrick, P. J. Data visualization for the characterization of naphthenic acids within petroleum samples. *Energy Fuels* **2009**, *23*, 2592−2599.
(44) Grewer, D. M.; Young, R. F.; Whittal, R. M.; Fedorak, P. M. Naphthenic acids and other acid-extractables in water samples from Alberta: What is being measured? *Sci. Total Environ.* **2010**, *408*, 5997−6010.
(45) Purcell, J. M.; Hendrickson, C. L.; Rodgers, R. P.; Marshall, A. G. Atmospheric pressure photoionization Fourier transform ion cyclotron resonance mass spectrometry for complex mixture analysis. *Anal. Chem.* **2006**, *78*, 5906−5912.
(46) Griffiths, M. T.; Da Campo, R.; O'Connor, P. B.; Barrow, M. P. Throwing light on petroleum: simulated exposure of crude oil to sunlight and characterization using atmospheric pressure photo-

DOI: 10.1021/acs.energyfuels.9b00469
Energy Fuels 2019, 33, 4420−4431

ionization Fourier transform ion cyclotron resonance mass spectrometry. *Anal. Chem.* **2014**, *86*, 527−534.
(47) Pereira, A. S.; Bhattacharjee, S.; Martin, J. W. Characterization of oil sands process-affected waters by liquid chromatography Orbitrap mass spectrometry. *Environ. Sci. Technol.* **2013**, *47*, 5504−5513.
(48) Yi, Y.; Birks, S. J.; Cho, S.; Gibson, J. J. Characterization of organic composition in snow and surface waters in the Athabasca Oil Sands Region, using ultrahigh resolution Fourier transform mass spectrometry. *Sci. Total Environ.* **2015**, *518-519*, 148−158.
(49) Rodgers, R. P.; Klein, G. C.; Wu, Z.; Marshall, A. G. Environmental applications of ESI FT-ICR Mass spectrometry: the identification of polar n, s and o containing PAH species in crude oil and coal extracts. *Prepr. Pap.—Am. Chem. Soc., Div. Fuel Chem.* **2003**, *48*, 758−759.
(50) Kim, Y. H.; Kim, S. Improved abundance sensitivity of molecular ions in positive-ion APCI MS analysis of petroleum in toluene. *J. Am. Soc. Mass Spectrom.* **2010**, *21*, 386−392.
(51) Purcell, J. M.; Hendrickson, C. L.; Rodgers, R. P.; Marshall, A. G. Atmospheric Pressure Photoionization Proton Transfer for Complex Organic Mixtures Investigated by Fourier Transform Ion Cyclotron Resonance Mass Spectrometry. *J. Am. Soc. Mass Spectrom.* **2007**, *18*, 1682−1689.
(52) Ajaero, C.; McMartin, D. W.; Peru, K. M.; Bailey, J.; Haakensen, M.; Friesen, V.; Martz, R.; Hughes, S. A.; Brown, C.; Chen, H.; McKenna, A. M.; Corilo, Y. E.; Headley, J. V. Fourier Transform Ion Cyclotron Resonance Mass Spectrometry Characterization of Athabasca Oil Sand Process-Affected Waters Incubated in the Presence of Wetland Plants. *Energy Fuels* **2017**, *31*, 1731−1740.
(53) Ajaero, C.; Peru, K. M.; Simair, M.; Friesen, V.; O'Sullivan, G.; Hughes, S. A.; McMartin, D. W.; Headley, J. V. Fate and behavior of oil sands naphthenic acids in a pilot-scale treatment wetland as characterized by negative-ion electrospray ionization orbitrap mass spectrometry. *Sci. Total Environ.* **2018**, *631-632*, 829−839.
(54) Kaiser, N. K.; Quinn, J. P.; Blakney, G. T.; Hendrickson, C. L.; Marshall, A. G. A Novel 9.4 Tesla FTICR Mass Spectrometer with Improved Sensitivity, Mass Resolution, and Mass Range. *J. Am. Soc. Mass Spectrom.* **2011**, *22*, 1343−1351.
(55) Blakney, G. T.; Hendrickson, C. L.; Marshall, A. G. Predator data station: A fast data acquisition system for advanced FT-ICR MS experiments. *Int. J. Mass Spectrom.* **2011**, *306*, 246−252.
(56) Wilcox, B. E.; Hendrickson, C. L.; Marshall, A. G. Improved ion extraction from a linear octopole ion trap: SIMION analysis and experimental demonstration. *J. Am. Soc. Mass Spectrom.* **2002**, *13*, 1304−1312.
(57) Kaiser, N. K.; Savory, J. J.; Hendrickson, C. L. Controlled ion ejection from an external trap for extended m/z range in FT-ICR mass spectrometry. *J. Am. Soc. Mass Spectrom.* **2014**, *25*, 943−949.
(58) Kaiser, N. K.; Savory, J. J.; McKenna, A. M.; Quinn, J. P.; Hendrickson, C. L.; Marshall, A. G. Electrically compensated Fourier transform ion cyclotron resonance cell for complex mixture mass analysis. *Anal. Chem.* **2011**, *83*, 6907−6910.
(59) Xian, F.; Hendrickson, C. L.; Blakney, G. T.; Beu, S. C.; Marshall, A. G. In *Broadband Phase Correction of Complex FT-ICR Mass Spectra, 1-5 June 2008, Denver, CO, 2008*; Proceedings 56th ASMS Conference on Mass Spectrometry & Allied Topics: Denver, CO, 2008; p TP008.
(60) Xian, F.; Hendrickson, C. L.; Blakney, G. T.; Beu, S. C.; Marshall, A. G. Automated Broadband Phase Correction of Fourier Transform Ion Cyclotron Resonance Mass Spectra. *Anal. Chem.* **2010**, *82*, 8807−8812.
(61) Xian, F.; Corilo, Y. E.; Hendrickson, C. L.; Marshall, A. G. Baseline correction of absorption-mode Fourier transform ion cyclotron resonance mass spectra. *Int. J. Mass Spectrom.* **2012**, *325-327*, 67−72.
(62) Ledford, E. B., Jr.; Rempel, D. L.; Gross, M. L. Space charge effects in Fourier transform mass spectrometry. II. Mass calibration. *Anal. Chem.* **1984**, *56*, 2744−2748.
(63) Shi, S. D.-H.; Drader, J. J.; Freitas, M. A.; Hendrickson, C. L.; Marshall, A. G. Comparison and interconversion of the two most common frequency-to-mass calibration functions for Fourier transform ion cyclotron resonance mass spectrometry. *Int. J. Mass Spectrom.* **2000**, *195-196*, 591−598.
(64) Kendrick, E. A Mass Scale Based on CH2= 14.0000 for High Resolution Mass Spectrometry of Organic Compounds. *Anal. Chem.* **1963**, *35*, 2146−2154.
(65) Hughey, C. A.; Hendrickson, C. L.; Rodgers, R. P.; Marshall, A. G.; Qian, K. Kendrick Mass Defect Spectrum: A Compact Visual Analysis for Ultrahigh-Resolution Broadband Mass Spectra. *Anal. Chem.* **2001**, *73*, 4676−4681.
(66) McLafferty, F. W.; Turecek, F. *Interpretation of Mass Spectra*, 4th ed.; University Science Books: Mill Valley, CA, 1993.
(67) Corilo, Y. E. *PetroOrg Software*; Florida State University, Omics LLC: Tallahassee, FL, 2014.
(68) Headley, J. V.; Peru, K. M.; Barrow, M. P. Mass spectrometric characterization of naphthenic acids in environmental samples: A review. *Mass Spectrom. Rev.* **2009**, *28*, 121−134.
(69) Yi, Y.; Han, J.; Jean Birks, S.; Borchers, C. H.; Gibson, J. J.; Gibson, J. J. Profiling of dissolved organic compounds in the oil sands region using complimentary liquid-liquid extraction and ultrahigh resolution Fourier transform mass spectrometry. *Environ. Earth Sci.* **2017**, *76*, 828.
(70) Wang, C.; Huang, R.; Klamerth, N.; Chelme-Ayala, P.; Gamal El-Din, M. Positive and negative electrospray ionization analyses of the organic fractions in raw and oxidized oil sands process-affected water. *Chemosphere* **2016**, *165*, 239−247.
(71) Aitken, C. M.; Jones, D. M.; Larter, S. R. Anaerobic hydrocarbon biodegradation in deep subsurface oil reservoirs. *Nature* **2004**, *431*, 291−294.
(72) Headley, J. V.; Peru, K. M.; Mohamed, M. H.; Wilson, L.; McMartin, D. W.; Mapolelo, M. M.; Lobodin, V. V.; Rodgers, R. P.; Marshall, A. G. Atmospheric pressure photoionization Fourier transform ion cyclotron resonance mass spectrometry characterization of tunable carbohydrate-based materials for sorption of oil sands naphthenic acids. *Energy Fuels* **2014**, *28*, 1611−1616.
(73) Mapolelo, M. M.; Rodgers, R. P.; Blakney, G. T.; Yen, A. T.; Asomaning, S.; Marshall, A. G. Characterization of naphthenic acids in crude oils and naphthenates by electrospray ionization FT-ICR mass spectrometry. *Int. J. Mass Spectrom.* **2011**, *300*, 149−157.
(74) Kim, S.; Stanford, L. A.; Rodgers, R. P.; Marshall, A. G.; Walters, C. C.; Qian, K.; Wenger, L. M.; Mankiewicz, P. Microbial alteration of the acidic and neutral polar NSO compounds revealed by Fourier transform ion cyclotron resonance mass spectrometry. *Org. Geochem.* **2005**, *36*, 1117−1134.
(75) Zhu, X.; Shi, Q.; Zhang, Y.; Pan, N.; Xu, C.; Chung, K. H.; Zhao, S. Characterization of Nitrogen Compounds in Coker Heavy Gas Oil and Its Subfractions by Liquid Chromatographic Separation Followed by Fourier Transform Ion Cyclotron Resonance Mass Spectrometry. *Energy Fuels* **2011**, *25*, 281−287.
(76) Yue, S.; Ramsay, B. A.; Brown, R. S.; Wang, J.; Ramsay, J. A. Identification of estrogenic compounds in oil sands process waters by effect directed analysis. *Environ. Sci. Technol.* **2015**, *49*, 570−577.
(77) Headley, J. V.; Barrow, M. P.; Peru, K. M.; Fahlman, B.; Frank, R. A.; Bickerton, G.; McMaster, M. E.; Parrott, J.; Hewitt, L. M. Preliminary fingerprinting of Athabasca oil sands polar organics in environmental samples using electrospray ionization Fourier transform ion cyclotron resonance mass spectrometry. *Rapid Commun. Mass Spectrom.* **2011**, *25*, 1899−1909.
(78) Meshref, M. N. A.; Chelme-Ayala, P.; Gamal El-Din, M. Fate and abundance of classical and heteroatomic naphthenic acid species after advanced oxidation processes: Insights and indicators of transformation and degradation. *Water Res.* **2017**, *125*, 62−71.
(79) Headley, J. V.; Peru, K. M.; Mohamed, M. H.; Wilson, L.; McMartin, D. W.; Mapolelo, M. M.; Lobodin, V. V.; Rodgers, R. P.; Marshall, A. G. Electrospray Ionization Fourier Transform Ion Cyclotron Resonance Mass Spectrometry Characterization of Tunable

DOI: 10.1021/acs.energyfuels.9b00469
Energy Fuels 2019, 33, 4420−4431

Carbohydrate-Based Materials for Sorption of Oil Sands Naphthenic Acids. *Energy Fuels* **2013**, *27*, 1772−1778.
(80) Pan, Y.; Liao, Y.; Shi, Q. Variations of Acidic Compounds in Crude Oil during Simulated Aerobic Biodegradation: Monitored by Semiquantitative Negative-Ion ESI FT-ICR MS. *Energy Fuels* **2017**, *31*, 1126−1135.
(81) Pereira, A. S.; Islam, M. S.; Gamal El-Din, M.; Martin, J. W. Ozonation degrades all detectable organic compound classes in oil sands process-affected water; an application of high-performance liquid chromatography/obitrap mass spectrometry. *Rapid Commun. Mass Spectrom.* **2013**, *27*, 2317−2326.
(82) Smith, D. F.; Schaub, T. M.; Kim, S.; Rodgers, R. P.; Rahimi, P.; Teclemariam, A.; Marshall, A. G. Characterization of Acidic Species in Athabasca Bitumen and Bitumen Heavy Vacuum Gas Oil by Negative-Ion ESI FT−ICR MS with and without Acid−Ion Exchange Resin Prefractionation. *Energy Fuels* **2008**, *22*, 2372−2378.
(83) Smith, D. F.; Rahimi, P.; Teclemariam, A.; Rodgers, R. P.; Marshall, A. G. Characterization of Athabasca bitumen heavy vacuum gas oil distillation cuts by negative/positive electrospray ionization and automated liquid injection field desorption ionization Fourier transform ion cyclotron resonance mass spectrometry. *Energy Fuels* **2008b**, *22*, 3118−3125.
(84) Tian, Y.; Chen, L.; Zhang, S.; Zhang, S. A systematic study of soluble microbial products and their fouling impacts in membrane bioreactors. *Chem. Eng. J.* **2011**, *168*, 1093−1102.
(85) Hwang, G.; Dong, T.; Islam, M. S.; Sheng, Z.; Pérez-Estrada, L. A.; Liu, Y.; Gamal El-Din, M. The Impacts of Ozonation on Oil Sands Process-Affected Water Biodegradability and Biofilm Formation Characteristics in Bioreactors. *Bioresour. Technol.* **2013**, *130*, 269−277.
(86) Barrow, M. P.; Peru, K. M.; McMartin, D. W.; Headley, J. V. Effects of Extraction pH on the Fourier Transform Ion Cyclotron Resonance Mass Spectrometry Profiles of Athabasca Oil Sands Process Water. *Energy Fuels* **2016**, *30*, 3615−3621.
(87) Shi, Q.; Hou, D.; Chung, K. H.; Xu, C.; Zhao, S.; Zhang, Y. Characterization of Heteroatom Compounds in a Crude Oil and Its Saturates, Aromatics, Resins, and Asphaltenes (SARA) and Non-basic Nitrogen Fractions Analyzed by Negative-Ion Electrospray Ionization Fourier Transform Ion Cyclotron Resonance Mass Spectrometry. *Energy Fuels* **2010**, *24*, 2545−2553.
(88) Imfeld, G.; Braeckevelt, M.; Kuschk, P.; Richnow, H. H. Monitoring and assessing processes of organic chemicals removal in constructed wetlands. *Chemosphere* **2009**, *74*, 349−362.
(89) Bedessem, M. E.; Ferro, A. M.; Hiegel, T. Pilot-Scale Constructed Wetlands for Petroleum-Contaminated Groundwater. *Water Environ. Res.* **2007**, *79*, 581−586.
(90) Liao, Y.; Shi, Q.; Hsu, C. S.; Pan, Y.; Zhang, Y. Distribution of acids and nitrogen-containing compounds in biodegraded oils of the Liaohe Basin by negative ion ESI FT-ICR MS. *Org. Geochem.* **2012**, *47*, 51−65.
(91) Toor, N. S.; Han, X.; Franz, E.; MacKinnon, M. D.; Martin, J. W.; Liber, K. Selective biodegradation of naphthenic acids and a probable link between mixture profiles and aquatic toxicity. *Environ. Toxicol. Chem.* **2013**, *32*, 2207−2216.

DOI: 10.1021/acs.energyfuels.9b00469
Energy Fuels 2019, 33, 4420−4431